

Compressed Sensing with Correlation Between Measurements and Noise

Thomas Arildsen, Torben Larsen

Abstract—Existing convex relaxation-based approaches to reconstruction in compressed sensing assume that noise in the measurements is independent of the measurements themselves. We consider the case of noise correlated with the compressed measurements and introduce a simple technique for improvement of compressed sensing reconstruction from such measurements. The technique is based on a linear model of the correlation of additive noise with the measurements. The modification of the reconstruction algorithm based on this model is very simple and has negligible additional computational cost compared to standard reconstruction algorithms. The proposed technique reduces reconstruction error considerably in the case of correlated measurements and noise. Numerical experiments confirm the efficacy of the technique. The technique is demonstrated with application to low-rate quantization of compressed measurements, which is known to introduce correlated noise, and improvements in reconstruction error up to approximately 7 dB are observed for 1 bit/sample quantization.

I. INTRODUCTION

IN the recently emerged field of compressed sensing, one considers linear measurements \mathbf{y} of a sparse vector \mathbf{x} , possibly affected by noise as:

$$\mathbf{y} = \mathbf{A}\mathbf{x} + \mathbf{n}, \quad (1)$$

where the measurements $\mathbf{y} \in \mathbb{R}^{M \times 1}$, the sparse vector $\mathbf{x} \in \mathbb{R}^{N \times 1}$, the additive noise $\mathbf{n} \in \mathbb{R}^{M \times 1}$, the system matrix $\mathbf{A} \in \mathbb{R}^{M \times N}$, and $M \ll N$ [1]–[3]. \mathbf{A} is generally the product of a measurement matrix and a dictionary matrix: $\mathbf{A} = \mathbf{\Phi}\mathbf{\Psi}$, where $\mathbf{\Phi} \in \mathbb{C}^{M \times N}$, $\mathbf{\Psi} \in \mathbb{C}^{N \times N}$. For simplicity, we assume that $\mathbf{\Psi}$ is an orthonormal basis although more general dictionaries are indeed possible [4].

The essence of compressed sensing, as Donoho, Candès, Romberg, and Tao show in [1], [2], is that the under-determined equation system (1) can be solved provided that:

- 1) The vector \mathbf{x} is sparse; i.e., only few (K) elements in \mathbf{x} are non-zero.

$$K = |\{x_i | x_i \neq 0, i = 1, \dots, N\}| \quad (2)$$

\mathbf{x} can also be approximated sparsely if it is compressible [3, Sec. 3.3], meaning that its coefficients sorted by magnitude decay rapidly to zero.

- 2) The system matrix \mathbf{A} obeys the Restricted Isometry Property (RIP) with isometry constant $\delta_K > 0$, defined as follows:

$$(1 - \delta_K) \|\mathbf{x}\|_{\ell_2}^2 \leq \|\mathbf{A}\mathbf{x}\|_{\ell_2}^2 \leq (1 + \delta_K) \|\mathbf{x}\|_{\ell_2}^2, \quad (3)$$

This work was partially financed by The Danish Council for Strategic Research under grant number 09-067056 and by the Danish Center for Scientific Computing.

The authors are with Aalborg University, Faculty of Engineering and Science, Department of Electronic Systems, DK-9220 Aalborg, Denmark, e-mail: {th|tl}@es.aau.dk.

for any at most K -sparse vector \mathbf{x} such that [5]:

$$\delta_K + \delta_{2K} + \delta_{3K} < 1. \quad (4)$$

This holds with high probability when $\mathbf{\Phi}$ is generated with zero-mean independent identically distributed (i.i.d.) Gaussian entries with variance $\frac{1}{M}$. Note that (3) and (4) are sufficient but not necessary conditions, and rather conservative conditions indeed, as shown in [6].

- 3) The measurement process captures a sufficient amount of measurements M [7]:

$$M \geq CK \log \left(\frac{N}{M} \right), \quad (5)$$

where C is a fairly small constant which can be calculated as a function of $\frac{M}{N}$ [5]. (5) holds for the Gaussian measurement matrices $\mathbf{\Phi}$ mentioned above.

Given the measurements \mathbf{y} , the unknown sparse vector \mathbf{x} can be reconstructed by solving the following convex optimization problem [8, Sec. 1.3]:

$$\hat{\mathbf{x}} = \underset{\mathbf{u}: \|\mathbf{y} - \mathbf{A}\mathbf{u}\|_2 \leq \epsilon}{\operatorname{argmin}} \|\mathbf{u}\|_1, \quad (6)$$

where the fidelity constraint $\|\mathbf{y} - \mathbf{A}\mathbf{u}\|_2 \leq \epsilon$ ensures consistency with the observed measurements to within some margin of error, ϵ , which is chosen sufficiently large to accommodate the error \mathbf{n} . The form of the optimization problem in (6) is known as Least Absolute Shrinkage and Selection Operator (LASSO) [9] or Basis Pursuit De-Noising (BPDN) [10] and also comes in other variants such as the Dantzig selector [11]. In addition to the convex optimization approach to reconstruction in compressed sensing, there exist several iterative/greedy algorithms such as Iterative Hard Thresholding (IHT) [12], or Subspace Pursuit (SP) [13] and Compressive Sampling Matching Pursuit (CoSaMP) [14] as well as the more generalized incarnation of the two latter, Two-Stage Thresholding (TST) [15]. We generally refer to such convex or greedy approaches as reconstruction algorithms. The reconstruction algorithms generally assume the noise to be white and independent of the noiseless measurements $\bar{\mathbf{y}} = \mathbf{A}\mathbf{x}$. In particular, to the best of the authors' knowledge, the case of measurement noise correlated with the measurements has not been treated in the existing literature. Such correlation arises in for example the case of low-resolution quantization. As we demonstrate in Section II, this case poses a problem for the accuracy of the found solution $\hat{\mathbf{x}}$.

In this paper, we propose a simple yet efficient approach to alleviating the problem of correlation between the noiseless measurements $\bar{\mathbf{y}}$ and the noise \mathbf{n} . Our proposal boils down to a simple scaling of the solution $\hat{\mathbf{x}}$. Through numerical

experiments we demonstrate how correlated measurements and noise adversely affect the reconstruction error and demonstrate how our proposal improves the estimates considerably.

As an application example, we demonstrate the proposed approach in the case of low-rate scalar quantization of the measurements $\bar{\mathbf{y}}$ which can be observed to introduce the mentioned correlated measurement noise. We demonstrate how a well-known linear model used for modeling such correlation in scalar quantization is equivalent to the model of correlated measurement noise considered in this work.

The article is structured as follows: Section II introduces the considered model of correlation between compressed measurements and noise and proposes a solution to enhance reconstruction under these conditions, Section III describes simulations conducted to evaluate the performance of the proposed approach compared to a traditional approach, Section IV presents the results of these numerical simulations, Section V provides discussions of some of the presented results, and Section VI concludes the article.

II. METHODOLOGY

A. Correlated Measurements and Noise

We consider additive measurement noise \mathbf{n} which is correlated with the measurements $\bar{\mathbf{y}}$. We model the correlation by the linear model:

$$\mathbf{y} = \alpha \mathbf{A} \mathbf{x} + \mathbf{w}, \quad (7)$$

where \mathbf{w} is assumed an additive white noise uncorrelated with \mathbf{x} and $0 < \alpha \leq 1$ where $\alpha = 1$ covers the ordinary case of uncorrelated measurement noise. \mathbf{A} is the product of a measurement matrix Φ with i.i.d. Gaussian entries $\sim \mathcal{N}(0, \frac{1}{M})$ and an orthonormal dictionary matrix Ψ . The model (7) results in the following additive noise term:

$$\mathbf{n} = \mathbf{y} - \bar{\mathbf{y}} \quad (8)$$

$$= \alpha \mathbf{A} \mathbf{x} + \mathbf{w} - \mathbf{A} \mathbf{x} \quad (9)$$

$$= (\alpha - 1) \mathbf{A} \mathbf{x} + \mathbf{w} \quad (10)$$

We define $\bar{\mathbf{y}} = \mathbf{A} \mathbf{x}$ to signify the measurements before introduction of additive noise. It is readily seen from (10) that \mathbf{n} is correlated with \mathbf{x} . The noise variance is

$$\sigma_n^2 = \frac{1}{M} \mathbb{E} [\mathbf{n}^T \mathbf{n}] = \frac{1}{M} ((\alpha - 1)^2 \mathbb{E} [\bar{\mathbf{y}}^T \bar{\mathbf{y}}] + \mathbb{E} [\mathbf{w}^T \mathbf{w}]), \quad (11)$$

which can be calculated by assuming that $\sigma_y^2 = \frac{1}{M} \mathbb{E} [\bar{\mathbf{y}}^T \bar{\mathbf{y}}]$ and $\sigma_w^2 = \frac{1}{M} \mathbb{E} [\mathbf{w}^T \mathbf{w}]$ are known or can be estimated. For example, we show in Section II-F how σ_y^2 can be estimated. Likewise, we show an example for σ_w^2 in the case of quantization in Section II-E, (23).

The specific problem caused by correlated measurements and noise as modeled by (7) is that the noise itself is partly sparse in the same dictionary as the signal of interest, \mathbf{x} . Intuitively, this causes a solution $\hat{\mathbf{x}}$ as given by, e.g., (6) to adapt to part of the noise *as well as* the signal of interest, unless steps are taken to mitigate this effect.

B. Proposed Approach

Using the model in (7), we propose the following reconstruction of the sparse vector \mathbf{x} instead of the standard approach in (6). Equation (7) motivates replacing the system matrix \mathbf{A} by its scaled version $\alpha \mathbf{A}$. We exemplify this approach by applying it in the BPDN reconstruction formulation as below. Replacing \mathbf{A} by $\alpha \mathbf{A}$ in the standard approach (6), we arrive at

$$\hat{\mathbf{x}}_1 = \underset{\mathbf{u}: \|\mathbf{y} - \alpha \mathbf{A} \mathbf{u}\|_2 \leq \epsilon}{\operatorname{argmin}} \|\mathbf{u}\|_1. \quad (12)$$

Since ϵ should be chosen to accommodate the level of noise in the measurements \mathbf{y} , we can see that, one choice could be to set

$$\epsilon = \|\mathbf{n}\|_2 \quad (13)$$

in (6), or

$$\epsilon = \|\mathbf{w}\|_2 \quad (14)$$

in (12). Since the noise terms \mathbf{n} and \mathbf{w} are assumed unknown, (13) and (14) are not realistic choices of ϵ . The optimal choice of ϵ is dependent on the true solution \mathbf{x} , and is therefore difficult to obtain in practice as exemplified for more general inverse problems in, e.g., [16]. For this reason, various rules of thumb exist for the selection of ϵ . One such choice is found in [17, Sec. 5.3]:

$$\epsilon = \sqrt{M + 2\sqrt{2M}}\sigma, \quad (15)$$

where σ is the noise level (standard deviation) of the stochastic error \mathbf{n} or \mathbf{w} in (1) or (7), respectively.

C. Additional Insight on the Proposed Approach

As outlined in Section II-B, the model of the correlation between \mathbf{n} and $\bar{\mathbf{y}}$ suggests scaling \mathbf{A} in the constraint of (12). In fact, as we show here, the same solution can be obtained simply by scaling the solution found by the optimization formulation (6).

Proposition 1. *The following optimization formulation is equivalent to the formulation (12), i.e. their solutions are identical:*

$$\hat{\mathbf{x}}_2 = \frac{1}{\alpha} \underset{\mathbf{v}: \|\mathbf{y} - \mathbf{A} \mathbf{v}\|_2 \leq \epsilon}{\operatorname{argmin}} \|\mathbf{v}\|_1. \quad (16)$$

To see why (16) is equivalent to (12), consider the optimization problem over the variable \mathbf{v}

$$\begin{aligned} \hat{\mathbf{x}}_2 &= \underset{\mathbf{v}: \|\mathbf{y} - \mathbf{A} \mathbf{v}\|_2 \leq \epsilon}{\operatorname{argmin}} \left\| \frac{1}{\alpha} \mathbf{v} \right\|_1 \\ &= \underset{\mathbf{u}: \|\mathbf{y} - \alpha \mathbf{A} \mathbf{u}\|_2 \leq \epsilon}{\operatorname{argmin}} \|\mathbf{u}\|_1, \quad \mathbf{v} = \alpha \mathbf{u} \\ &= \hat{\mathbf{x}}_1 \end{aligned} \quad (17)$$

The equalities in (17) hold since the solutions to the optimization problems are unique under the conditions of sparsity of \mathbf{x} and RIP of \mathbf{A} [7]. Thus, down-scaling the solution to the optimization in (16) by α results in the same solution $\hat{\mathbf{x}}_2$ as the solution $\hat{\mathbf{x}}_1$ to (12). Please note that all constraints in

(12), (16) and (17) use the same value of ϵ given by (15) with $\sigma = \sigma_w$, the standard deviation of the entries in \mathbf{w} in (7).

In short, Proposition 1 says that for compressed measurements with noise correlated with the measurements according to the model (7), given the correlation parameter α , when the signal \mathbf{x} is reconstructed using BPDN, (6), the obtained solution should be scaled by the factor $\frac{1}{\alpha}$ to account for the effect of the correlation.

Proposition 1 has been verified through simulations comparing the solutions (12) and (16). Numerical results of this verification are presented in Section IV-B.

D. Optimality of the Proposed Approach

In relation to the method proposed in Sections II-B and II-C, it is of course interesting to investigate whether the corrective scaling by α in the reconstruction of \mathbf{x} is indeed optimal. To investigate this, consider the following optimization formulation:

$$\hat{\mathbf{x}}_\beta = \frac{1}{\beta} \underset{\mathbf{u}: \|\mathbf{y} - \mathbf{A}\Psi\mathbf{u}\|_2 \leq \epsilon}{\operatorname{argmin}} \|\mathbf{u}\|_1, \quad (18)$$

where ϵ is given by (15) and the optimization problem is evaluated for a number of values of $\beta \in [\alpha - \beta_1, \alpha + \beta_2]$ for a given value of α used in the correlated noise model (7) and a suitable choice of β_1 and β_2 . The numerical results of this investigation can be found in Section IV-C. $\beta = \alpha$ intuitively seems a suitable choice, but numerical experiments indicate that it is in fact not optimal. An explanation of this observation is offered in Section V.

E. An Application: Quantization

As a practical example where the introduced measurement noise is correlated with the measurements, we investigate low-rate scalar quantization of the individual compressed measurements in \mathbf{y} . Quantization is usually modeled by an additive noise model [18]:

$$y = Q(\bar{y}) = \bar{y} + q, \quad (19)$$

where \bar{y} is the original value before quantization, which we consider as $\bar{y} \in \mathbb{R}$. $Q(\cdot)$ is the (non-linear) operation of scalar quantization, mapping \bar{y} to an index i representing a quantized value y

$$Q: \bar{y} \rightarrow y_i, \text{ if } \bar{y} \in R_i, i \in \{1, \dots, L\}, \quad (20)$$

where the range of input values is partitioned into L regions R_i , $i \in \{1, \dots, L\}$ and any value $\bar{y} \in R_i$ is quantized to the point $y_i \in R_i$. For input \bar{y} with unbounded support, the regions R_i can be defined as follows:

$$R_i = \begin{cases} (p_{i-1}, p_i], & \text{for } i = 1, \dots, L-1 \\ (p_{L-1}, p_L], & \text{for } i = L, \end{cases} \quad (21)$$

where $p_0 = -\infty \wedge p_L = \infty$. The additive noise $q = y - \bar{y}$ represents the error introduced by quantizing \bar{y} to the value y .

Various modeling assumptions are typically made about q . One type of quantizers has centroid codebooks, i.e. quantizers where the reconstruction points y_i are calculated as the

respective centroids of the distribution of the input y in each of the regions R_i , e.g., Lloyd-Max quantizers [19], [20]. For quantizers with centroid codebooks, q is correlated with the input x . A model of this correlation used in the literature is the so-called gain-plus-additive-noise model [21, Sec. II]:

$$y = Q(\bar{y}) = \alpha \bar{y} + r, \quad (22)$$

where $\alpha \in [0, 1]$ and r is an additive noise, assumed uncorrelated with \bar{y} . The variance of r is

$$\sigma_r^2 = \alpha(1 - \alpha)\sigma_{\bar{y}}^2. \quad (23)$$

The variance of q is

$$\sigma_q^2 = (1 - \alpha)\sigma_{\bar{y}}^2, \quad (24)$$

which is easily seen by inserting (23) in $\sigma_q^2 = (\alpha - 1)^2\sigma_{\bar{y}}^2 + \sigma_r^2$.

The parameter α can be computed for a specific quantizer. One way to do this is to estimate it empirically by Monte-Carlo simulation. From [21, Eq. (8)] we have

$$\alpha = 1 - \frac{\sigma_q^2}{\sigma_{\bar{y}}^2}. \quad (25)$$

The procedure is to generate a random test sequence \bar{y} , quantize it with the given quantizer Q designed¹ for the p.d.f. of \bar{y} , estimate the variances σ_q^2 and $\sigma_{\bar{y}}^2$ from the realizations of \bar{y} and $q = \bar{y} - y$, and use these to calculate (25).

The model (22) of the quantizer corresponds to the proposed model of correlated measurements and noise described by (7), where $r = w$. Please note that the model, (22), considers scalar quantization. In the case of quantization of a vector \mathbf{v} , we use $Q(\mathbf{v})$ to signify scalar quantization of the individual elements of the vector \mathbf{v} .

We consider quantization of compressed measurements \mathbf{y} of the signal \mathbf{x} :

$$\mathbf{y} = Q(\mathbf{A}\mathbf{x}) \quad (26)$$

$$= \mathbf{A}\mathbf{x} + \mathbf{q} \quad (27)$$

$$\approx \alpha \mathbf{A}\mathbf{x} + \mathbf{w}, \quad (28)$$

where

$$\mathbb{E}[\mathbf{q}\mathbf{q}^T] = \sigma_q^2 \mathbf{I}, \quad \mathbb{E}[\bar{\mathbf{y}}\bar{\mathbf{y}}^T] = \sigma_{\bar{y}}^2 \mathbf{I},$$

and \mathbf{I} is the $M \times M$ identity matrix.

Approximating the quantization operation by the noise model in (28), we propose using the reconstruction technique (16) to improve reconstruction with scalar quantized compressed measurements, (26), as an example of noise correlated with the measurements.

F. Estimates of Noise Variance

Provided that \mathbf{x} is known to be sparse with K non-zero elements, and \mathbf{A} obeys the RIP with some constant δ_K , $\sigma_{\bar{\mathbf{y}}}^2$ can be approximated, requiring only knowledge of K and the p.d.f. of the non-zero entries in \mathbf{x} . If we assume that the individual

¹The quantizer can for example be trained on test data representing \bar{y} or calculated based on the known or assumed probability density function (p.d.f.) of \bar{y} .

non-zero entries in \mathbf{x} are distributed i.i.d. Gaussian $\sim \mathcal{N}(0, 1)$, we have

$$\begin{aligned} \mathbb{E} [\bar{\mathbf{y}}^T \bar{\mathbf{y}}] &= \mathbb{E} [\mathbf{x}^T \mathbf{A}^T \mathbf{A} \mathbf{x}] = \mathbb{E} [\|\mathbf{A} \mathbf{x}\|_2^2] \\ &\approx \mathbb{E} [\|\mathbf{x}\|_2^2], \end{aligned} \quad (29)$$

where the approximation in (29) follows from (3). Since the non-zero entries of \mathbf{x} are i.i.d. Gaussian distributed, $\|\mathbf{x}\|_2^2$ is χ^2 -distributed with K degrees of freedom [22, Sec. 8.7.2]. This leads to:

$$\mathbb{E} [\bar{\mathbf{y}}^T \bar{\mathbf{y}}] \approx K. \quad (30)$$

Estimates of the corresponding noise variances follow from (23) and (24).

When K is unknown, noise variance estimates given by (23) and (24) can be obtained from a known σ_y^2 . In hardware implementations, σ_y^2 can be considered known through the use of automatic gain control prior to quantization or by other means of estimating signal variance prior to quantization.

III. SIMULATION FRAMEWORK

In this section we present the numerical simulation set-up used to evaluate the reconstruction method proposed in (16).

Donoho & Tanner have shown in [6] that compressed sensing problems can be divided into two “phases” according to their probability of correct recovery by the method (6). When evaluating the probability of correct reconstruction of a sparse vector \mathbf{x} over the parameter space defined by $\delta = \frac{M}{N} \in [0, 1]$ and $\rho = \frac{K}{M} \in [0, 1]$, a given problem can be proven to fall into one of two phases where the probability of correct reconstruction is close to 1 (feasible) and 0 (infeasible), respectively. These two phases are divided by a sharp phase transition around the correct reconstruction probability of 50% as drawn in Fig. 1 (—). The feasible phase lies below the transition and the infeasible phase lies above. Compressed sensing is utilized most efficiently when operating close to the phase transition in the feasible phase since \mathbf{x} can be reconstructed with the highest possible number of non-zero elements K , given N and M , here. This phase transition occurs in the case of noiseless measurements, in the limit of $N \rightarrow \infty$. The theory still holds for finite N , but the phase transition is shifted downwards with respect to ρ in the (δ, ρ) -parameter space, see Fig. 1 (- - -). It has also been shown that a similar transition occurs at the same location in the noisy case, i.e. (1) [23]. In the noisy case, the squared norm of the reconstruction error, $\|\hat{\mathbf{x}} - \mathbf{x}\|_2^2$ relative to the measurement noise variance σ_n^2 is bounded in the feasible region and unbounded in the infeasible region.

In all simulations, we apply the proposed approach to test signals generated randomly according to the following specifications: size of \mathbf{x} vector $N = 1000$; number of compressed measurements $M \in \{200, 300, 400, 500, 600, 700, 800, 900, 1000\}$. The non-zero elements of \mathbf{x} are i.i.d. $\sim \mathcal{N}(0, 1)$; the number of non-zero elements K is selected for each value of M . This is done by calculating the largest possible K for each M according to the lower bound on the 99% phase transition for finite $N = 1000$ by the formula given in [6,

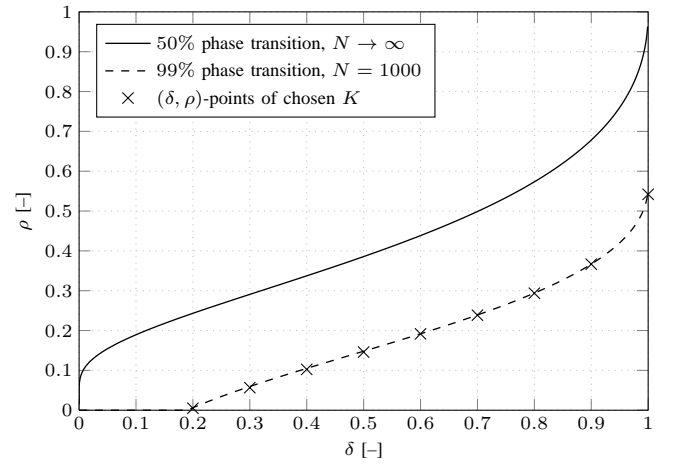


Fig. 1. The theoretical Donoho-Tanner phase transition for $N \rightarrow \infty$, lower bound for $N = 1000$, and points corresponding to the values of K chosen for test signals.

Sec. IV, Theorem 2], drawn in Fig. 1 (- - -). The resulting values are $K \in \{1, 17, 41, 73, 115, 167, 235, 330, 542\}$. The corresponding (δ, ρ) -points are plotted in Fig. 1 (x).

The measurement matrix Φ has i.i.d. entries $\sim \mathcal{N}(0, \frac{1}{M})$ and we use the dictionary $\Psi = \mathbf{I}$, so that $\mathbf{A} = \Phi$. We repeat the experiment $T = 1000$ times for randomly generated \mathbf{x} and Φ in each repetition and average the reconstructed signal Normalized Mean Squared Error (NMSE), \mathcal{P} , over all solution instances $\hat{\mathbf{x}}_i$, $i \in [1, T]$:

$$\mathcal{P} = \sum_{i=1}^T \frac{\|\hat{\mathbf{x}}_i - \mathbf{x}_i\|_2^2}{\|\mathbf{x}_i\|_2^2}. \quad (31)$$

To enable assessment of the quality of the obtained results, we plot the simulated figures with error bars signifying their 95% confidence intervals computed under the assumption of a Gaussian distributed mean of the NMSE, see e.g. [24, Sec. 7.3.1]. The simulations were conducted for reconstruction using regular BPDN (6) vs. our proposed approach (16). The numerical optimization problems were solved using the SPGL1² software package [25].

Regarding the choice of ϵ , for regular BPDN (6), we chose ϵ according to (15), with $\sigma = \sqrt{\sigma_q^2}$ from (24). For our proposed approach (16), we chose ϵ according to (15), with $\sigma = \sqrt{\sigma_r^2}$ from (23). For both compared approaches, we consider σ_y^2 known. As demonstrated in Section IV-C, ϵ could be chosen better from empirical observations to provide smaller error in the reconstruction, i.e. $\|\hat{\mathbf{x}} - \mathbf{x}\|$. We chose the values (15) as practically useful values for fairness of the evaluation of our proposed method.

All scripts required to reproduce the simulation results are openly accessible³.

IV. NUMERICAL SIMULATION RESULTS

In this section we present results of the numerical simulations conducted according to Section III. Firstly, we evaluate

²SPGL1: A solver for large-scale sparse reconstruction (<http://www.cs.ubc.ca/labs/scl/spgl1>).

³<http://github.com/ThomasA/cs-correlated-noise>

TABLE I
CORRELATION PARAMETER VALUES USED IN FIGS. 2–4.

Equiv. quantizer resolution	α (Lloyd-Max)	α (uniform)
1 bit/sample	0.6366	0.6366
3 bit/sample	0.9655	0.9626
5 bit/sample	0.9975	0.9965

the proposed method under artificial correlated measurement noise generated according to (7). Secondly, we evaluate the method under correlated measurement noise incurred by scalar quantization of the compressed measurements. These results are shown in Section IV-A. Furthermore, we present results of simulations conducted to assess the validity of Proposition 1 in Section IV-B as well as results in Section IV-C to shed light on how the choices of the parameters β and ϵ in (18) affect the main results.

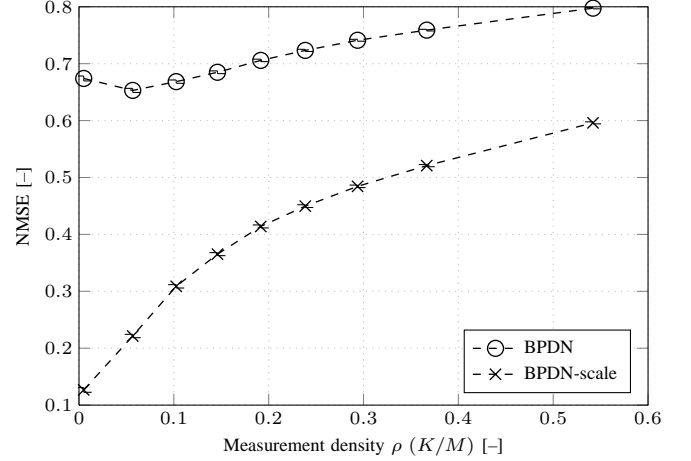
A. Main Results

In this section, noise variance and correlation parameters are first set equal to the corresponding parameters estimated for the Lloyd-Max quantizer used later in this section, for comparability. The parameter values for α are listed in Table I. The listed values of α (Lloyd-Max) are used together with σ_r^2 calculated from (23) to generate correlated measurement noise according to (7). In the conducted simulations, BPDN is used to reconstruct \hat{x}_2 from the compressed measurements \mathbf{y} . We compare the standard (correlation-unaware) reconstruction, (6), of the signal (denoted “BPDN” in Fig. 2) to the reconstruction obtained by our proposed method, (16), of scaling the reconstructed signal to account for correlation (denoted “BPDN-scale” in Fig. 2). Selected results for equivalent quantizer resolutions 1 bit/sample, 3 bit/sample, and 5 bit/sample are shown in Fig. 2. The proposed method is observed to improve the reconstruction error \mathcal{P} by 7.3 dB to 1.3 dB (for increasing ρ) at 1 bit/sample, 3.1 dB to 0.26 dB (for increasing ρ) at 3 bit/sample, and 0.86 dB to 0.059 dB (for increasing ρ) at 5 bit/sample.

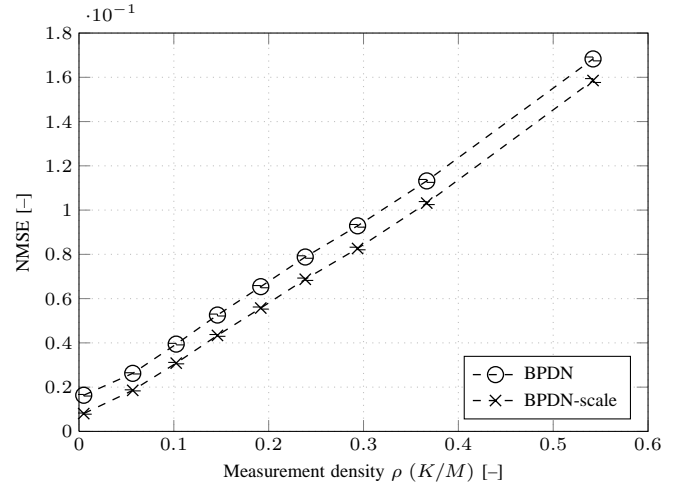
The experiments for quantized measurements are conducted exactly as above, with the exception that the measurements \mathbf{y} are quantized using a *Lloyd-Max quantizer* [19], [20]. The correlated noise model uses the values of α (Lloyd-Max) for the selected quantizer resolutions listed in Table I.

Selected results for quantizer resolutions 1 bit/sample, 3 bit/sample, and 5 bit/sample with Lloyd-Max quantization are shown in Fig. 3. It can be observed that the reconstruction error figures \mathcal{P} agree well with those simulated with artificially generated correlated noise in Fig. 2. The observed improvements by the proposed method are almost identical to those observed for artificial noise: 7.6 dB to 1.3 dB at 1 bit/sample, 3.1 dB to 0.26 dB at 3 bit/sample, and 0.80 dB to 0.028 dB at 5 bit/sample.

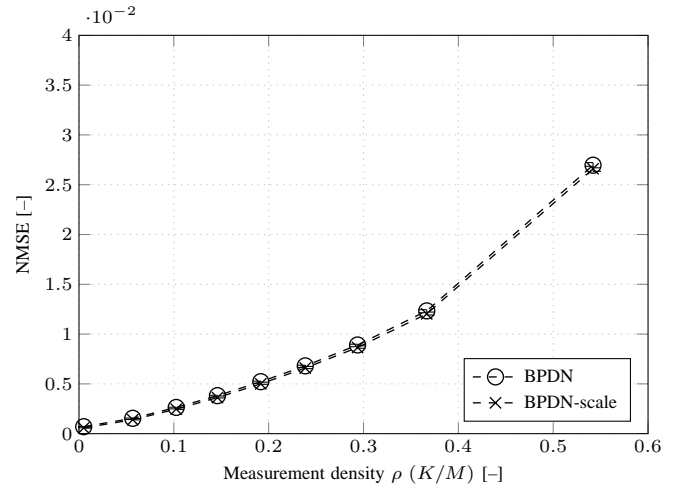
To evaluate our proposed approach for a more practical quantization scheme than the non-uniform Lloyd-Max quantizer, we additionally simulated results where the measurements \mathbf{y} are quantized using a uniform quantizer with mid-point quantization points, optimized for minimum mean squared error (MMSE) of the quantized measurements. This



(a) Noise of var. equivalent to 1 bit/sample quantizer.



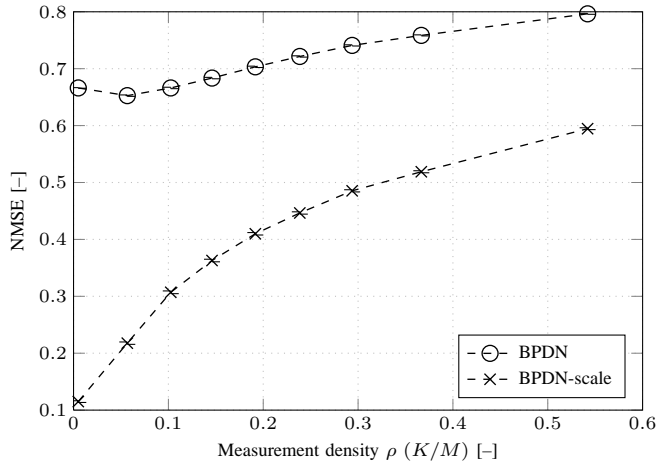
(b) Noise of var. equivalent to 3 bit/sample quantizer.



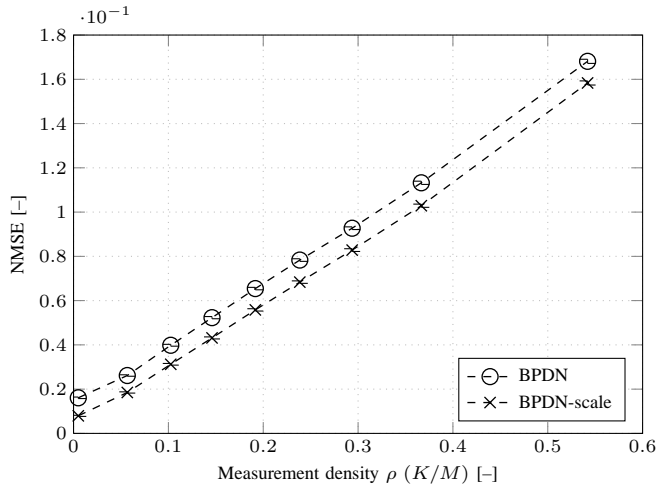
(c) Noise of var. equivalent to 5 bit/sample quantizer.

Fig. 2. Simulated NMSE of reconstruction using BPDN vs. relative number of measurements for parameters α and σ_r^2 set equal to the corresponding values for Lloyd-Max quantizers at the respective rates specified under figures (a)–(c).

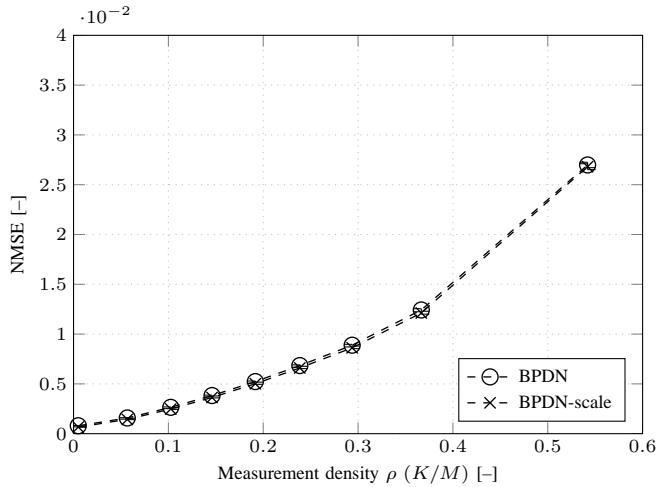
serves to evaluate how well the proposed approach performs for a more practical quantizer type that does not theoretically obey the quantization noise model (22) due to the fact that



(a) 1 bit/sample quantizer.



(b) 3 bit/sample quantizer.



(c) 5 bit/sample quantizer.

Fig. 3. Simulated NMSE of reconstruction using BPDN vs. relative number of measurements for parameters α and σ_r^2 set equal to the corresponding values for Lloyd-Max quantizers at the respective rates specified under figures (a)-(c).

its reconstruction points are not the centroids of the input signal's p.d.f. in the quantizer's input regions. The correlated noise model uses the values of α (uniform) from Table I.

Selected results for quantizer resolutions 1 bit/sample, 3 bit/sample, and 5 bit/sample with uniform quantization are shown in Fig. 4. The observed improvements by the proposed method are close to those observed for artificial noise: 7.6 dB to 1.3 dB at 1 bit/sample, 3.2 dB to 0.28 dB at 3 bit/sample, and 0.89 dB to 0.073 dB at 5 bit/sample. The results in Fig. 3a and 4a are identical due to the fact that the 2-level Lloyd-Max quantizer is a uniform 2-level quantizer optimized for MMSE of the quantized values. It can also be observed that the uniform quantizer for 3 bit/sample and 5 bit/sample results in slightly larger reconstruction error while the improvement by our proposed method is preserved.

B. Empirical Assessment of Validity of Proposition 1

To empirically assess the validity of Proposition 1, the experiments in Section IV-A for synthetic correlated noise have been repeated using the reconstruction method (12). The resulting estimates $\hat{\mathbf{x}}_1$ were then compared to the corresponding estimates $\hat{\mathbf{x}}_2$. In other words, this experiment evaluates the difference in the solutions found by scaling the measurement matrix Φ by α prior to reconstruction as opposed to scaling solutions $\hat{\mathbf{x}}$ by $1/\alpha$ after reconstruction.

For each signal realization and instance of K and M , the norm of the error between the two estimates is evaluated:

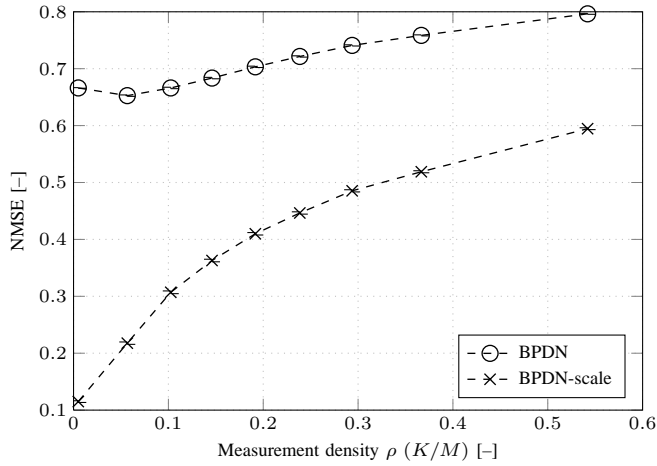
$$e = \|\hat{\mathbf{x}}_1 - \hat{\mathbf{x}}_2\|_2 \quad (32)$$

For the experiments with random noise in Section IV-A, we observed a total of 87 instances where $e > 10^{-6}$. This is a fraction of $87/27000 = 0.32\%$ of the total number of signal realizations. For the experiments with Lloyd-Max quantization, we observed a total of 77 instances where $e > 10^{-6}$. This is a fraction of $77/27000 = 0.29\%$ of the total number of signal realizations. The observed distributions of errors $e > 10^{-6}$ corresponding to the experiments behind Figs. 2 and 3 are shown in Figs. 5 and 6.

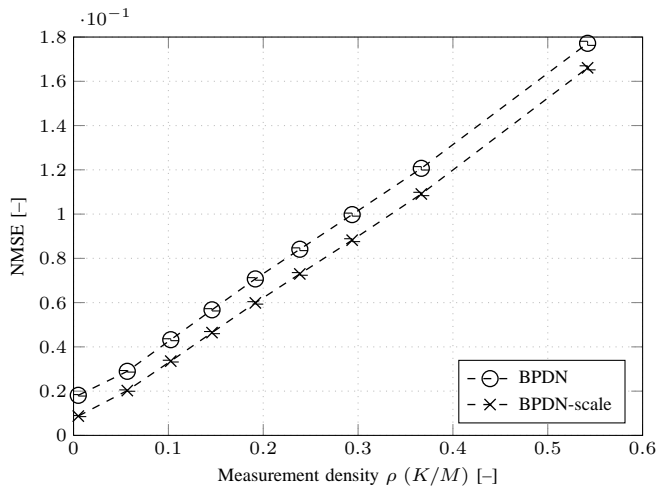
C. Empirical Investigation of Scaling Factors and Regularization Parameters

In order to assess the optimality of the proposed approach as described in Section II-D, we conducted simulations for values of β in (18) using artificial pseudo-random noise generated according to the model (22). Since the reconstruction error performance is also affected by the choice of ϵ in (18), we similarly performed the simulations over different values ϵ . Preliminary simulations indicated that \mathcal{P} (see (31)) evolves in a quasi-convex manner over β and ϵ . Based on this observation, we have used the Nelder-Mead simplex algorithm [26] to find the (β, ϵ) -optimal error figures \mathcal{P} for each of the points (M, K) with correlated noise generated according to each of the values α (Lloyd-Max) in Table I are shown in Table II. The optimal regularization parameter values for ordinary BPDN are denoted ϵ_1 , while the optimal scaling and regularization parameter values for the proposed method are denoted β_2 and ϵ_2 .

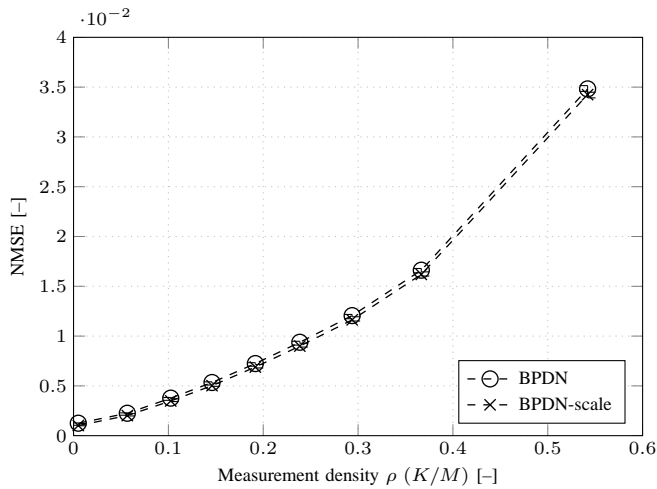
It was expected that α would be the optimal choice of β , i.e. $\beta = \alpha$. However, it turns out that the (empirically observed)



(a) 1 bit/sample quantizer.



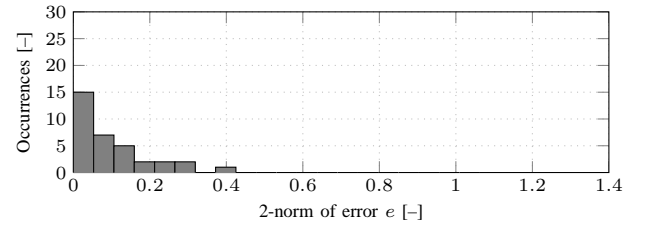
(b) 3 bit/sample quantizer.



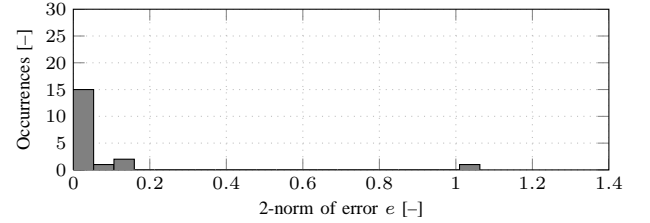
(c) 5 bit/sample quantizer.

Fig. 4. Simulated NMSE of reconstruction using BPDN vs. relative number of measurements for parameters α and σ_r^2 set equal to the corresponding values for uniform quantizers at the respective rates specified under figures (a)-(c).

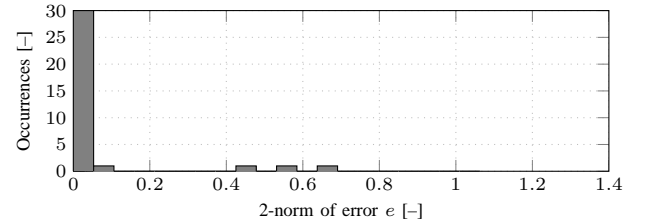
optimal value of β_2 is typically slightly smaller than α with observed values $\beta_2 \in [0.74\alpha, 0.98\alpha]$, depending on (M, K) . An exception is seen in Table IIIa, where $\beta_2 \in [1.0\alpha, 1.2\alpha]$.



(a) Equivalent to 1 bit/sample quantizer.



(b) Equivalent to 3 bit/sample quantizer.



(c) Equivalent to 5 bit/sample quantizer.

Fig. 5. Histograms of observed discrepancies, $e > 1 \cdot 10^{-6}$ between the proposed methods in (12) and (16) in the experiments with synthetic noise in Section IV-A.

The optimal values of the regularization parameter ϵ are similarly found to be lower than the values given by (15). For the baseline method (6), the (empirically observed) optimal values are observed as $\epsilon_1 \in [0.32\epsilon, 0.84\epsilon]$, depending on (M, K) , where ϵ denotes the values given by (15) as described in Section III. For our proposed method (16), the optimal values are generally closer to the values given by (15) with observed values $\epsilon_1 \in [0.45\epsilon, 1.0\epsilon]$, depending on (M, K) .

It is important to note that the demonstrated advantage of our proposed approach in Section IV-A is not merely a result of a particularly lucky choice of ϵ , as these experiments testify. The observed NMSE of our proposed method, \mathcal{P}_2 , consistently outperforms the baseline approach, \mathcal{P}_1 . The improvement is consistent across different correlation parameters α as seen in Table II where \mathcal{P}_2 is smaller than \mathcal{P}_1 by 13 dB, 11 dB and 7.1 dB in Tables IIIa–IIIc, respectively, for $(M, K) = (200, 1)$. At the other extreme of $(M, K) = (1000, 542)$, \mathcal{P}_2 is smaller than \mathcal{P}_1 by 0.14 dB, 0.18 dB and 0.19 dB, respectively.

V. DISCUSSION

It was shown in Section IV-B that there were a few discrepancies found in the conducted simulations for which Proposition 1 did not hold within an error $e < 10^{-6}$. These occurrences were found to be very rare and we attribute these to effects of numerical precision in the reconstruction.

As seen from the experimental results in Section IV-C, the correlation parameter α from (7) may in fact not be the optimal

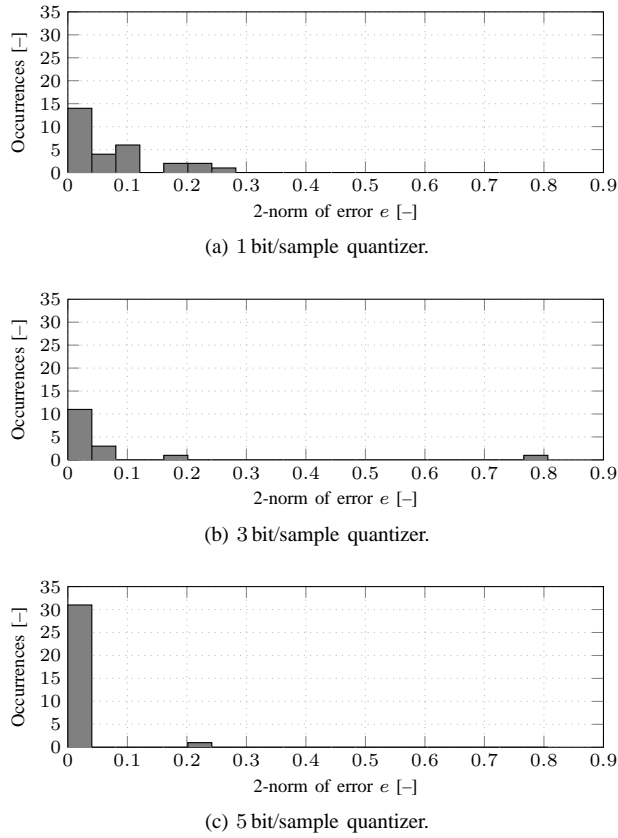


Fig. 6. Histograms of observed discrepancies, $e > 1 \cdot 10^{-6}$ between the proposed methods in (12) and (16) in the experiments with quantization noise in Section IV-A.

choice of scaling parameter, as expressed by β in (18). The generally smaller values found in Section IV-C to be optimal for BPDN reconstruction according to (18) can be explained by the fact that they scale the estimate $\hat{\mathbf{x}}_\beta$ larger. It is well-known in the literature that the ℓ_1 -norm minimization approach represented by, e.g., (6) tends to penalize larger coefficients of \mathbf{x} more than smaller coefficients [27], thus estimating the former relatively too small. Therefore, it is possible to choose a scaling parameter $\beta < \alpha$ in (18) that improves the estimate $\hat{\mathbf{x}}_\beta$, i.e. yields smaller $\|\hat{\mathbf{x}}_\beta - \mathbf{x}\|$ compared to $\|\hat{\mathbf{x}}_\alpha - \mathbf{x}\|$. At this time, we cannot quantify the optimal β analytically and it depends on the indeterminacy and/or measurement density of the performed compressed sensing.

VI. CONCLUSION

We proposed a simple technique to model correlation between measurements and an additive noise in compressed sensing signal reconstruction. The technique is based on a linear model of the correlation between the measurements and noise. It consists of scaling signals reconstructed by a well-known ℓ_1 -norm convex optimization method according to the model and comes at negligible computational cost. We provided practical expressions for computing the scaling parameter and the reconstruction regularization parameter.

We performed numerical simulations to demonstrate the obtainable reconstruction error improvement by the proposed method compared to ordinary ℓ_1 -norm convex optimization

TABLE II
SIMULATED NMSE AT EMPIRICALLY OPTIMAL PARAMETER VALUES β AND ϵ .

(M, K)	ϵ_1/ϵ	\mathcal{P}_1	β_2/α	ϵ_2/ϵ	\mathcal{P}_2
(200, 1)	0.64	$1.9 \cdot 10^{-2}$	0.85	0.91	$1.0 \cdot 10^{-3}$
(300, 17)	0.60	$3.3 \cdot 10^{-2}$	0.74	0.95	$1.3 \cdot 10^{-2}$
(400, 41)	0.55	$3.9 \cdot 10^{-2}$	0.78	0.92	$2.2 \cdot 10^{-2}$
(500, 73)	0.49	$4.2 \cdot 10^{-2}$	0.84	0.90	$2.9 \cdot 10^{-2}$
(600, 115)	0.53	$4.5 \cdot 10^{-2}$	0.87	0.84	$3.4 \cdot 10^{-2}$
(700, 167)	0.51	$4.7 \cdot 10^{-2}$	1.0	0.80	$3.9 \cdot 10^{-2}$
(800, 235)	0.48	$4.8 \cdot 10^{-2}$	1.0	0.77	$4.2 \cdot 10^{-2}$
(900, 330)	0.50	$4.9 \cdot 10^{-2}$	1.1	0.73	$4.5 \cdot 10^{-2}$
(1000, 542)	0.43	$5.3 \cdot 10^{-2}$	1.2	0.68	$5.1 \cdot 10^{-2}$

(a) Equivalent to 1 bit/sample quantizer.

(M, K)	ϵ_1/ϵ	\mathcal{P}_1	β_2/α	ϵ_2/ϵ	\mathcal{P}_2
(200, 1)	0.82	$4.8 \cdot 10^{-4}$	0.90	1.0	$4.2 \cdot 10^{-5}$
(300, 17)	0.75	$1.9 \cdot 10^{-3}$	0.94	0.84	$9.1 \cdot 10^{-4}$
(400, 41)	0.65	$3.0 \cdot 10^{-3}$	0.91	0.88	$1.7 \cdot 10^{-3}$
(500, 73)	0.64	$3.9 \cdot 10^{-3}$	0.90	0.89	$2.7 \cdot 10^{-3}$
(600, 115)	0.62	$4.8 \cdot 10^{-3}$	0.90	0.76	$3.5 \cdot 10^{-3}$
(700, 167)	0.62	$5.7 \cdot 10^{-3}$	0.93	0.69	$4.5 \cdot 10^{-3}$
(800, 235)	0.55	$6.5 \cdot 10^{-3}$	0.90	0.72	$5.5 \cdot 10^{-3}$
(900, 330)	0.50	$7.5 \cdot 10^{-3}$	0.93	0.62	$6.7 \cdot 10^{-3}$
(1000, 542)	0.49	$1.1 \cdot 10^{-2}$	0.97	0.50	$1.0 \cdot 10^{-2}$

(b) Equivalent to 3 bit/sample quantizer.

(M, K)	ϵ_1/ϵ	\mathcal{P}_1	β_2/α	ϵ_2/ϵ	\mathcal{P}_2
(200, 1)	0.84	$1.7 \cdot 10^{-5}$	0.98	1.0	$3.4 \cdot 10^{-6}$
(300, 17)	0.79	$1.2 \cdot 10^{-4}$	0.98	0.90	$6.0 \cdot 10^{-5}$
(400, 41)	0.68	$2.0 \cdot 10^{-4}$	0.97	0.94	$1.3 \cdot 10^{-4}$
(500, 73)	0.64	$2.8 \cdot 10^{-4}$	0.97	0.81	$1.9 \cdot 10^{-4}$
(600, 115)	0.60	$3.8 \cdot 10^{-4}$	0.97	0.75	$2.8 \cdot 10^{-4}$
(700, 167)	0.60	$4.7 \cdot 10^{-4}$	0.97	0.71	$3.6 \cdot 10^{-4}$
(800, 235)	0.58	$5.7 \cdot 10^{-4}$	0.97	0.67	$4.7 \cdot 10^{-4}$
(900, 330)	0.50	$7.3 \cdot 10^{-4}$	0.97	0.56	$6.4 \cdot 10^{-4}$
(1000, 542)	0.32	$1.3 \cdot 10^{-3}$	0.98	0.45	$1.3 \cdot 10^{-3}$

(c) Equivalent to 5 bit/sample quantizer.

reconstruction for noise generated according to the model. We further demonstrated as an example that the model applies well to low-rate scalar quantization of the measurements; both Lloyd-Max quantization that complies accurately with the correlation model, as well as a more practical uniform quantization. For example, simulations indicated that the proposed method offers improvements on the order of 1 dB to 7 dB for 1 bit/sample quantization, depending on the indeterminacy of the performed compressed sensing.

We conducted numerical simulations to evaluate the validity of our results which confirm that the improvements offered by the proposed method are not merely a coincidental result of the suggested practical choices of scaling and optimization regularization parameters. These results further indicated that the proposed method is robust to the choice of scaling and optimization regularization parameter in the sense that a sub-optimal choice still leads to considerable improvements over the ordinary convex optimization reconstruction method.

REFERENCES

- [1] D. Donoho, "Compressed sensing," *IEEE Transactions on Information Theory*, vol. 52, no. 4, pp. 1289–1306, Apr. 2006.

- [2] E. J. Candès, J. Romberg, and T. Tao, "Robust uncertainty principles: exact signal reconstruction from highly incomplete frequency information," *IEEE Transactions on Information Theory*, vol. 52, no. 2, pp. 489–509, Feb. 2006.
- [3] E. J. Candès, "Compressive sampling," in *Proceedings of the International Congress of Mathematicians*, vol. 3, 2006, pp. 1433–1452.
- [4] E. J. Candès, Y. C. Eldar, D. Needell, and P. Randall, "Compressed sensing with coherent and redundant dictionaries," *Applied and Computational Harmonic Analysis*, vol. 31, no. 1, pp. 59–73, 2011.
- [5] E. J. Candès and T. Tao, "Decoding by linear programming," *IEEE Transactions on Information Theory*, vol. 51, no. 12, pp. 4203–4215, Dec. 2005.
- [6] D. Donoho and J. Tanner, "Precise undersampling theorems," *Proceedings of the IEEE*, vol. 98, no. 6, pp. 913–924, Jun. 2010.
- [7] E. J. Candès and T. Tao, "Near-optimal signal recovery from random projections: Universal encoding strategies?" *IEEE Transactions on Information Theory*, vol. 52, no. 12, pp. 5406–5425, Dec. 2006.
- [8] S. Boyd and L. Vandenberghe, *Convex Optimization*. Cambridge: Cambridge University Press, 2004.
- [9] R. Tibshirani, "Regression shrinkage and selection via the lasso," *Journal of the Royal Statistical Society. Series B (Methodological)*, vol. 58, no. 1, pp. 267–288, 1996.
- [10] S. S. Chen, D. L. Donoho, and M. A. Saunders, "Atomic decomposition by basis pursuit," *SIAM Journal on Scientific Computing*, vol. 20, no. 1, pp. 33–61, 1998. [Online]. Available: <http://link.aip.org/link/?SCE/20/33/1>
- [11] E. Candès and T. Tao, "The dantzig selector: Statistical estimation when p is much larger than n ," *Annals of Statistics*, vol. 35, no. 6, pp. 2313–2351, 2007.
- [12] T. Blumensath and M. Davies, "Normalized iterative hard thresholding: Guaranteed stability and performance," *IEEE Journal of Selected Topics in Signal Processing*, vol. 4, no. 2, pp. 298–309, Apr. 2010.
- [13] W. Dai and O. Milenkovic, "Subspace pursuit for compressive sensing signal reconstruction," *IEEE Transactions on Information Theory*, vol. 55, no. 5, pp. 2230–2249, May 2009.
- [14] D. Needell and J. A. Tropp, "Cosamp: Iterative signal recovery from incomplete and inaccurate samples," *Applied and Computational Harmonic Analysis*, vol. 26, no. 3, pp. 301–321, 2009.
- [15] A. Maleki and D. Donoho, "Optimally tuned iterative reconstruction algorithms for compressed sensing," *IEEE Journal of Selected Topics in Signal Processing*, vol. 4, no. 2, pp. 330–341, Apr. 2010.
- [16] P. C. Hansen, *Rank-Deficient and Discrete Ill-Posed Problems: Numerical Aspects of Linear Inversion (Monographs on Mathematical Modeling and Computation)*. Philadelphia: Society for Industrial Mathematics, 1987.
- [17] S. Becker, J. Bobin, and E. J. Candès, "Nesta: A fast and accurate first-order method for sparse recovery," *SIAM Journal on Imaging Sciences*, vol. 4, no. 1, pp. 1–39, 2011.
- [18] N. S. Jayant and P. Noll, *Digital Coding of Waveforms - Principles and Applications to Speech and Video*. Englewood Cliffs, New Jersey: Prentice Hall, 1984.
- [19] S. Lloyd, "Least squares quantization in PCM," *IEEE Transactions on Information Theory*, vol. 28, no. 2, pp. 129–137, 1982, the material in this paper was presented in part at the Institute of Mathematical Statistics Meeting, Atlantic City, NJ, September 10–13, 1957.
- [20] J. Max, "Quantizing for minimum distortion," *IEEE Transactions on Information Theory*, vol. 6, no. 1, pp. 7–12, 1960.
- [21] P. H. Westerink, J. Biemond, and D. E. Boeke, "Scalar quantization error analysis for image subband coding using qmfs," *IEEE Transactions on Signal Processing*, vol. 40, no. 2, pp. 421–428, 2 1992.
- [22] K. S. Shanmugan and A. M. Breipohl, *Random Signals: Detection, Estimation and Data Analysis*. New York: Wiley, 1988.
- [23] D. Donoho, A. Maleki, and A. Montanari, "The noise-sensitivity phase transition in compressed sensing," *IEEE Transactions on Information Theory*, vol. 57, no. 10, pp. 6920–6941, Oct. 2011.
- [24] S. M. Ross, *Introduction to Probability and Statistics for Engineers and Scientists*, 2nd ed. San Diego: Academic Press, 2000.
- [25] E. van den Berg and M. P. Friedlander, "Probing the pareto frontier for basis pursuit solutions," *SIAM Journal on Scientific Computing*, vol. 31, no. 2, pp. 890–912, 2008. [Online]. Available: <http://link.aip.org/link/?SCE/31/890>
- [26] J. A. Nelder and R. Mead, "A simplex method for function minimization," *The Computer Journal*, vol. 7, no. 4, pp. 308–313, 1965. [Online]. Available: <http://comjnl.oxfordjournals.org/content/7/4/308.abstract>
- [27] E. Candès, M. Wakin, and S. Boyd, "Enhancing sparsity by reweighted ℓ_1 minimization," *Journal of Fourier Analysis and Applications*, vol. 14, no. 5, pp. 877–905, 2008.